Abstract: Engineered bamboo construction can be affected by natural defects, insects, corrosion, etc., which will result in damaging the mechanical properties of structural components. However, traditional reinforcement methods such as setting steel supports and increasing the cross-sectional area of components may cost a lot and cause a negative influence on the appearance of building. Many engineering practices and research works show that applying FRP (Fiber Reinforced Polymer/Fiber) sheet is an economical and efficient method for reinforcing and retrofitting building structures. Therefore, the compressive performance of AFRP (Aramid Fiber Reinforced Polymer/Fiber) reinforced laminated bamboo lumber (LBL) stub columns was studied in this paper. Through 6 groups (3 replicates for each group) of stub columns with 6 different cloth ratios, the influence of AFRP on the failure pattern and mechanical properties of bamboo columns was explored. The test results showed that AFRP could effectively restrain the lateral deformation and improve the mechanical behavior of LBL columns. With the increase in cloth ratio, the ultimate strength and elastic modulus increased linearly in general, while the Poisson's ratio gradually decreased. The reduced modulus of reinforced columns in the elastoplastic stage increased up to 161.31% compared with normal columns. Although the ductility of LBL columns laterally wrapped by AFRP was greatly improved, the initial stiffness, yield point and turning points between elastoplastic stage and plastic stage basically remained unchanged in contrast to unreinforced columns. Based on the test results, an empirical equation considering the cloth ratio was proposed to calculate the ultimate strength of AFRP reinforced LBL columns, using 'Lam and Teng' model. In addition, a simplified equation was also proposed to calculate the compressive strength of reinforced LBL columns derived from Mises yield criterion. The results of this work can be a reference to promote the application of strengthening and retrofitting engineered bamboo structure with FRP.

Keywords: Laminated bamboo; stub column; FRP; ultimate strength; reinforcement

1 Introduction

As a green building material in line with the concept of sustainable development, engineered bamboo has gradually attracted extensive attention from scholars [1-8]. It has distinct characteristics: on the one hand, engineered bamboo has the features of light weight, high strength along the grain direction [9] and environment friendly; on the other hand, engineered bamboo is a biological material, which can be affected by its own natural defects [10-11], bacteria, insects, temperature [12-13], high humidity [14-15] and corrosion, resulting in damaging the mechanical properties of bamboo structures. The demand for maintenance and retrofitting may be frequent. Traditional reinforcement methods, such as replacing structural members directly, setting steel supports, increasing the cross-sectional area of components, may affect the appearance of the building significantly. Therefore, there is an urgent need for a new method suitable for bamboo structures.

Many engineering practices and research works [16-18] show that FRP reinforcement is an economical and efficient method compared with traditional reinforcement methods. Due to the

decrease in cost of FRP and the increasing demand for reinforcing building structures all over the world, the method of strengthening building structures with FRP materials has become popular. Research works of FRP reinforced timber structures [19-24] can be references for engineered bamboo structures.

Najm et al. [19] conducted an experimental investigation of circular columns made of poplar wood confined with carbon fibers in an inorganic matrix and subjected to axial compression. The results showed that carbon fiber confinement increased strength, stiffness, ductility, and reduced the variability in timber column behavior under axial loads. Considering the effect of slenderness ratio, boundary conditions and FRP reinforcement length, Taheri et al. [20] investigated glulam timber columns strengthened with FRP under axial load. It was found that FRP laminates could offer incremental increase in the strength and stiffness of glulam columns. Kim et al. [21] formulated a three-dimensional finite element model to predict the behavior of timber beams strengthened with CFRP, and found an optimal CFRP-reinforcement ratio beyond which no strength increase was achieved. Zhang et al. [22] studied the compressive behavior of longitudinally cracked timber columns retrofitted using FRP sheets. It was showed that wrapping FRP sheets around cracked timber columns can recover their load-carrying capacity by up to 20%. Premrov et al. [23] used CFRP to reinforce timber-concrete composite beam, and emphasized that the presented concept of reinforcing was recommended only for strengthening old timber floor structures to assure a higher load-bearing capacity. Rescalvo et al. [24] conducted an experimental and analytical analysis for bending load capacity of old timber beams with defects when reinforced with carbon fiber strips. The reinforcement was evident for beams with natural defects and many years in service, with an improvement of up to 88% in bending load capacity.

According to the above literature review, it can be concluded that FRP can effectively improve the mechanical behavior of timber structures. As a bio-based material similar to wood, it's foreseeable that FRP can also have a positive influence on engineered bamboo structures. However, there are few studies on FRP reinforced bamboo structure so far. Zhang et al. [25] studied the AFRP influence on parallel bamboo strand lumber (PBSL) beams. They found that AFRP could increase the stiffness and ductility of bamboo beam, but reinforcement cannot increase the deflection of bamboo beams indefinitely. Wang et al. [26] examined the effect of slenderness ratio on AFRP reinforced laminated bamboo lumber columns, and proposed two equations to predict the ultimate load. These two preliminary works proved the positive influence of FRP on engineered bamboo, whilst the number of tests is far from enough to form a comprehensive cognition.

AFRP is made by mixing aramid fabrics with epoxy resin and hardener in a certain proportion, which has the characteristics of high strength, light weight, corrosion resistance, convenient construction, good durability [27]. Toutanji et al. [28] studied the strength and durability performance of concrete axially loaded members confined with AFRP composite sheets, and found that specimens wrapped with aramid fibers experienced no reduction in strength due to

wet/dry exposure. It is possible to improve the performance of engineered bamboo structure as well by combining AFRP with bamboo structure. Thus, we choose AFRP to study the compressive performance of reinforced laminated bamboo stub columns. In the present work, AFRP was laterally wrapped on laminated bamboo stub column, which was different from the works conducted by Zhang et al. [25] and Wang et al. [26]. According to six different cloth ratios, a total number of 18 stub columns were designed and tested to explore the effects of AFRP over failure mode, load-displacement behavior, strain-strain behavior, ultimate compressive strength, Poisson's ratio and elastic modulus. Based on the test results and Lam and Teng model, an empirical equation considering the cloth ratio was proposed to calculate the ultimate strength of AFRP reinforced LBL columns. In addition, a simplified equation was also proposed to calculate the compressive strength of reinforced LBL columns on the basis of Mises yield criterion. The results of this work can be a reference to promote the application of strengthening and retrofitting engineered bamboo structure with FRP.

2 Materials and methods

2.1 Non-reinforced LBL stub column

In this paper, LBL stub columns were all produced by Ganzhou Sentai Bamboo Wood Co. Ltd. With moso bamboo from Yongan, Fujian as raw material and resorcinol as adhesive, under the pressure of 9 MPa for upper and lower surfaces and 6.5 MPa for the left and right surfaces, bamboo laminates were hot pressed together in 157 ℃ condition for about 15 minutes. The moisture content and density of LBL in the test were 7.0% and 736 kg/m^3 respectively.

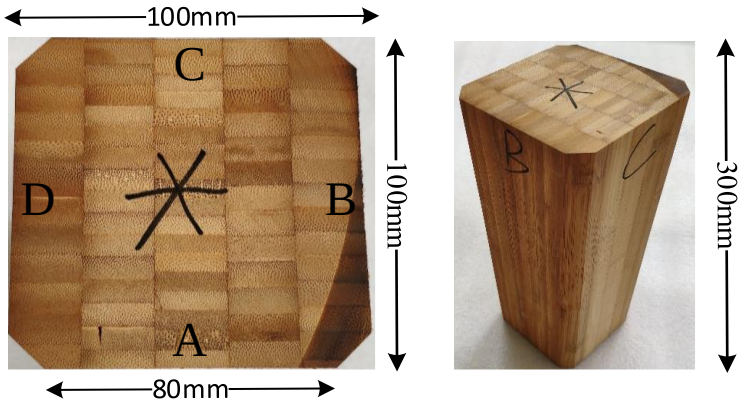

Figure 1 Original LBL column

The width *b* and height *h* of cross section were designed as 100 mm. The length of columns was set as 300mm. The arrangement of bamboo laminates and the cross-sectional shape of LBL columns are shown in Fig. 1. Due to the sudden change of the shape at the corners of rectangular section, the glued AFRP tended to bulge at the corners after drying and hardening. To avoid this, four chamfer of 10 mm in size were cut at the corners. All the columns took the wide surface of the bamboo strip as side A, and marked the remaining surfaces as side B, C and D successively along the counterclockwise direction. The top surface was denoted with ✳ and the bottom surface was blank.

2.2 AFRP reinforced LBL stub column

The epoxy resin 'SANYU RESIN L-500' selected in the test was from Shanghai Sanyu Rec Co. Ltd., which was composed of main agent L-500a and hardener L-500b in the ratio of 2:1. After the epoxy resin was proportioned, it was evenly coated on the AFRP cloth, and then the AFRP cloth was horizontally wrapped on LBL stub column (see Fig. 2a). The reinforced specimens were put at ambient temperature for one month. The tests were carried out after the epoxy resin was dried and hardened and AFRP sheets were fully bonded to columns. The mechanical and physical properties of AFRP are listed in Table 1 [25].

Table 1 Material properties and and main composition of AFRP

Elastic modulus	Ultimate tensile strength	thickness
202.64 GPa	1893.56 MPa	0.192 mm
	Main composition	
Aramid fabric	Epoxy resin	Hardener

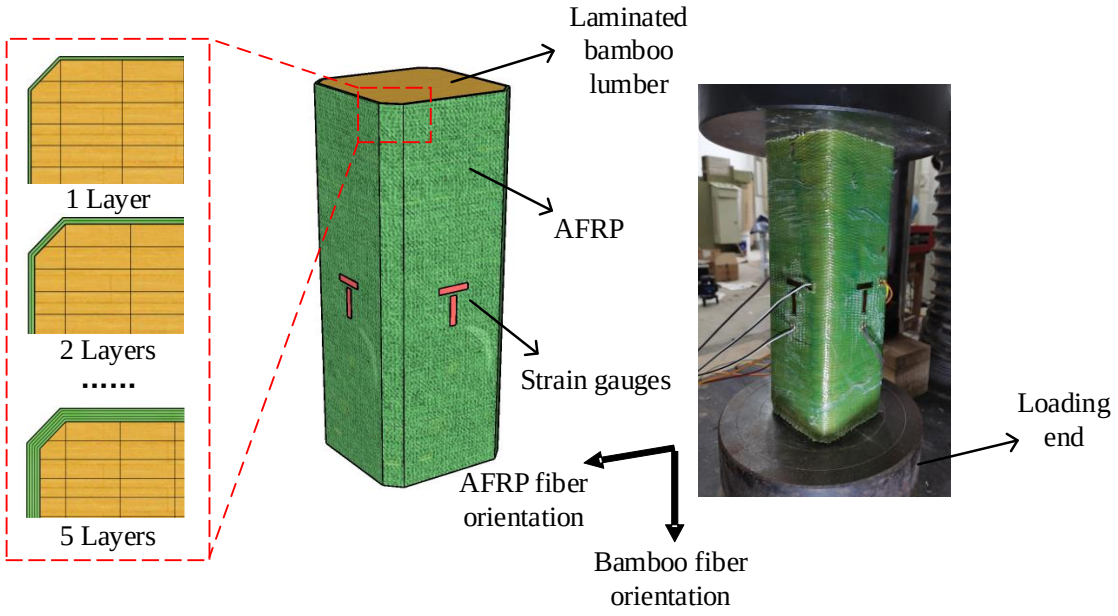

Figure 2(a) Schematic diagram of AFRP wrapping and (b) Physical diagram of test setup

A total number of 18 LBL stub columns (6 groups, 3 replicates for each group) were designed according to the number of AFRP layer i.e. 0~5 layers. Each layer of AFRP completely wrapped the specimen. 0~5 layers are related to six different cloth ratios of 0%, 0.74%, 1.48%, 2.21%, 2.95% and 3.69%, respectively. The equation for calculating cloth ratio in this study is as follows:

$$\rho = \frac{A_{FRP}}{A_c} = \frac{nt_f\left(2b+2h+4\sqrt{2}r-8r\right)}{bh-2r^2}\times 100\% \quad (1)$$

where A_{FRP} is cross-sectional area of FRP; A_c is cross-sectional area of laminated bamboo; n is number of FRP layer; t_f is thickness of FRP; b and h are width and height of cross section, respectively; r is size of chamfer. The expression in parentheses is the perimeter of the section. The names of specimens are shown in Table 2, where A300 is the reference group with no

reinforcement, SA2A300 means the bamboo column reinforced with two layers of AFRP.

Table 2 Detailed parameters of specimens

Group	Length	Number of specimens	Number of AFRP layer	ρ
A300	300mm	3	0	0%
SA1A300		3	1	0.74%
SA2A300		3	2	1.48%
SA3A300		3	3	2.21%
SA4A300		3	4	2.95%
SA5A300		3	5	3.69%

According to the standard for test methods of timber structures (GB/T 50329-2012), the loading system was designed. The physical diagram of the test is shown in Fig. 2b. The upper end was fixed and the lower end was spherical hinge support. A 200 t microcomputer controlled electro-hydraulic servo universal testing machine was selected for the test. The axial displacement of the specimen was measured by a displacement meter. Lateral and vertical strain gauges were applied at the mid-height of the four side surfaces to observe the change of strain. A TDS-540 data acquisition instrument was used for data collection. Load control was adopted in the initial stage of loading, and displacement control was used when the load reached 80% of the ultimate load. The time duration from initial loading to failure was controlled within 5~10 minutes.

3 Test results and analysis

3.1 Failure pattern of LBL stub column

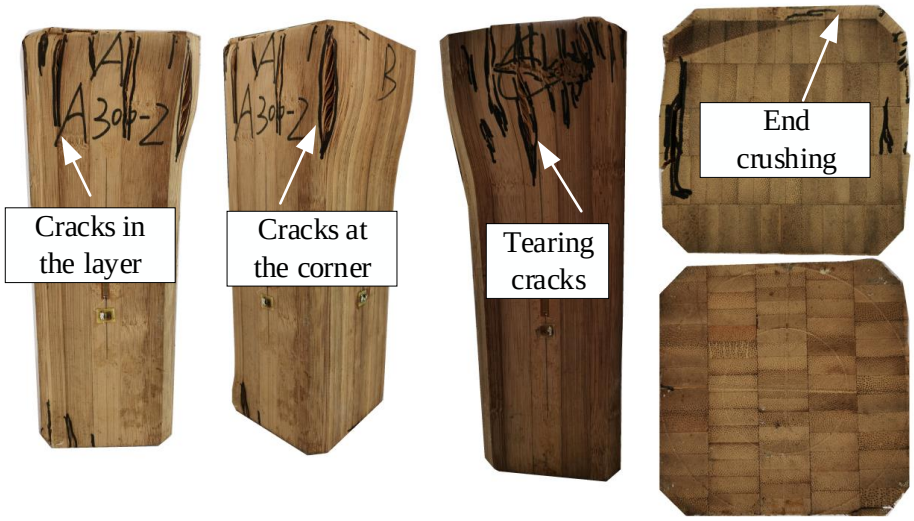

(a) Unreinforced LBL column

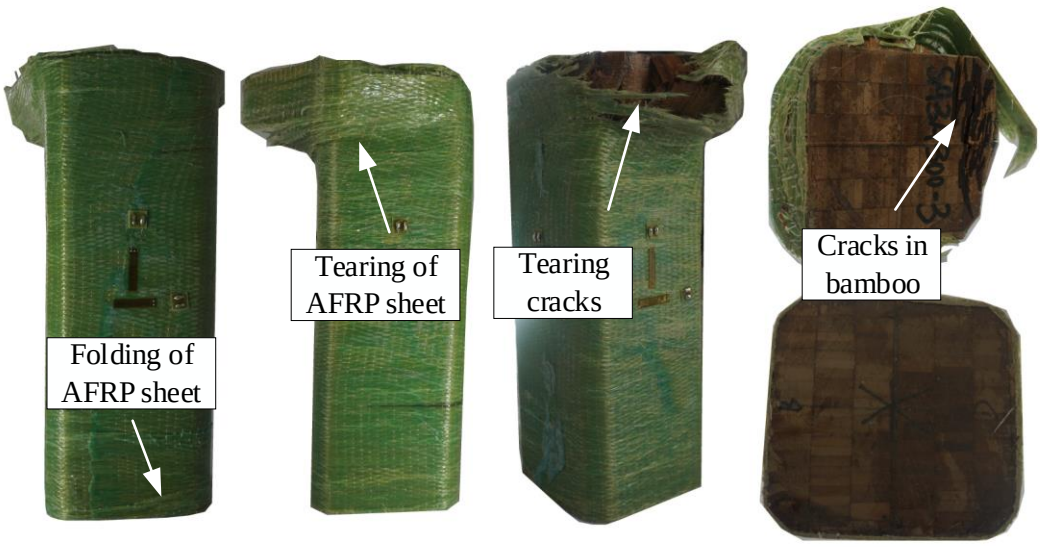

(b) AFRP reinforced LBL column

Figure 3 Typical failure pattern

Typical compressive failure patterns of laminated bamboo stub columns are shown in Figure 3. The unreinforced specimens were generally characterized by end crushing with local adhesive damage and bamboo strips cracking. During the initial loading, there was no obvious phenomenon on the surface of columns. As the load increased, the bamboo fibers at both ends of the specimens gradually became wrinkled, while the overall deformation of specimens remained insignificant. The bamboo strips and adhesive layers at the end began to crack when the specimens entered the plastic flow stage, and the cracking positions gradually increased with the increase of deformation degree, resulting in the loss of ultimate bearing capacity.

The failure process of short columns confined by FRP was similar to that of unreinforced specimens in the elastic and elastic-plastic stages. In the elastic-plastic stage, it was obvious that the AFRP cloth was folded in the perpendicular-to-the-fiber direction. When the plastic flow stage was reached, the FRP tore as the deformation increased. Unlike the unreinforced specimens, no visual crushing damage occurred at the end of the specimens. It was the bamboo strips that cracked apparently. FRP significantly limited the process of expanding the end of specimen outwards under compression.

3.2 Main test results

The main test results of 18 columns are shown in Table 3, where P_{max} is ultimate load; f_c is ultimate compressive strength; μ_{AC} and μ_{BD} are Poisson's ratio on in A/C plane and B/D plane, respectively; E_1 is the initial elastic modulus; E_2 is secant modulus calculated by yield point and ultimate strength point. Strength index 1 was calculated by compressive strength of reinforced specimen divided by that of unreinforced specimen, while strength index 2 was calculated by secant modulus of reinforced specimen divided by that of unreinforced specimen. Retainment ratio was calculated by E_2/E_1. Except for the Poisson's ratio and secant modulus, all other test data showed relevant coefficient of variation (COV) less than 20%, which indicates

that the test data are reliable. More discrete results of Poisson's ratio and secant modulus in Group SA1A300~SA5A300 were caused by unstable strain values during the folding of AFRP sheet.

According to the two strength indexes and retainment ratio, it is clear that the use of AFRP can increase the compressive strength and reduced modulus of LBL columns. The ultimate compressive strength went up to 70.6 MPa with an increasement of 24%, while the reduced modulus went up to 2438 MPa with an increasement of 161%. In the following sections, the average test results were used to analyze the impact of AFRP on mechanical properties of LBL columns in more detail.

Table 3 Main test results

Group	P_{max} /kN	f_c /MPa	Strength Index 1 (SI1)	μ_{AC}	μ_{BD}	E_1 /MPa	E_2 /MPa	Strength Index 2 (SI2)	Retainment ratio
A300-1	536.1	54.7		0.34	0.33	9365	1085		
A300-2	573.3	58.5		0.31	0.25	9197	737		
A300-3	563.8	57.5	1	0.34	0.26	9119	978	1	0.10
Mean	557.7	56.9		0.33	0.28	9227	933		
COV	2.83%	2.83%		4.29%	12.71%	1.11%	15.6%		
SA1A300-1	599.0	61.1		0.28	0.23	10385	2049		
SA1A300-2	628.2	64.1		0.28	0.17	9752	1036		
SA1A300-3	624.2	63.7	1.11	0.22	0.39	15175	1830	1.76	0.14
Mean	617.1	63.0		0.26	0.26	11771	1638		
COV	2.09%	2.11%		10.88%	35.71%	20.57%	26.57%		
SA2A300-1	618.4	63.1		0.30	0.31	9785	3123		
SA2A300-2	626.3	64.0		0.32	0.31	14250	3221		
SA2A300-3	630.8	64.4	1.12	0.27	0.24	10202	969	2.61	0.21
Mean	625.2	63.8		0.30	0.29	11412	2438		
COV	0.82%	0.85%		6.85%	11.38%	17.65%	42.63%		
SA3A300-1	613.3	62.6		0.22	0.29	9832	2570		
SA3A300-2	632.6	64.6		0.23	0.22	10125	2171		
SA3A300-3	639.6	65.3	1.13	0.24	0.39	11186	2394	2.55	0.23
Mean	629.2	64.2		0.23	0.3	10381	2378		
COV	1.77%	1.78%		3.55%	23.25%	5.60%	6.87%		
SA4A300-1	680.1	69.4		0.15	0.17	11185	1420		
SA4A300-2	693.2	70.7		0.26	0.22	13112	2913		
SA4A300-3	702.2	71.7	1.24	0.25	0.30	15409	2739	2.53	0.18
Mean	691.8	70.6		0.22	0.23	13235	2357		
COV	1.31%	1.33%		22.58%	23.27%	13.05%	28.28%		
SA5A300-1	674.5	68.8		0.20	0.18	10898	1872		
SA5A300-2	693.1	70.7		0.20	0.25	10614	2232		
SA5A300-3	656.8	67.0	1.21	0.21	0.21	10693	2444	2.34	0.20
Mean	674.8	68.9		0.20	0.21	10735	2183		
COV	2.2%	2.19%		2.36%	13.65%	1.11%	10.82%		

3.3 Effect of AFRP on mechanical properties

3.3.1 Load-displacement curves

Fig. 4 shows compared results of load vs axial displacement curves of specimens with different cloth ratio. The curves can be divided into four stages, i.e., elastic stage, elastoplastic stage, plastic stage and descending stage. In the elastic stage, the axial deformation increased linearly with the increase in load. Although the slope of curves decreased in the elastoplastic stage, the slope could be approximately considered as a constant value. At this stage, laminated bamboo yielded and some slight folds could be observed on AFRP sheets. In the plastic stage, obvious deformation could be observed. The specimens were compressed heavily and AFRP sheets were fractured. Finally, due to a large number of cracks inside the laminated bamboo, the bearing capacity of specimens was lost, and the tests were terminated.

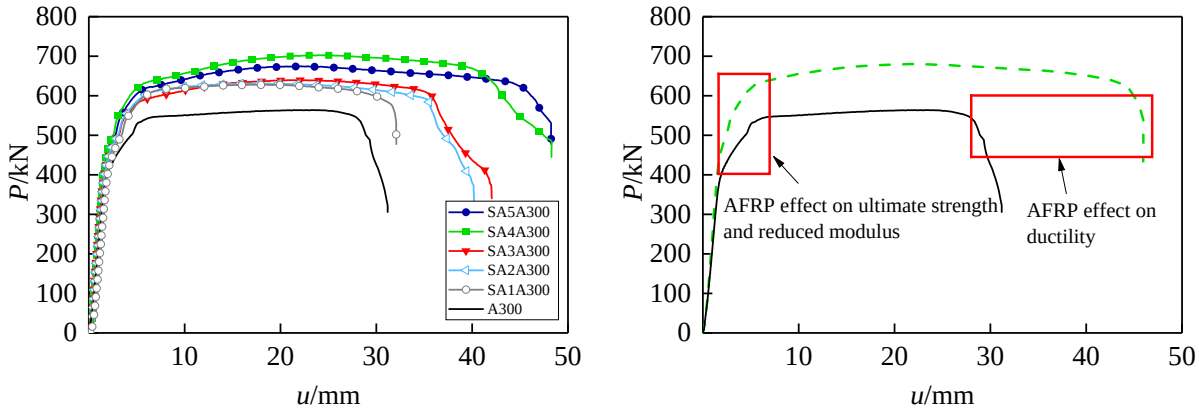

(a) Load-displacement response under different cloth ratio (b) AFRP influence on mechanical behavior

Figure 4 Load-displacement curves

3.3.2 Stress-strain curves and constitutive model

Fig. 5 shows stress vs strain curves of specimens with different cloth ratio. The whole stress-strain curves were derived from load-displacement curves, since the strain gauges pasted on specimens were damaged during the increasing of load. It can be seen from the Figure 4b that cloth ratio didn't have a great impact on the initial stiffness and elastic modulus. The reason is that the thickness and the transverse elastic modulus of AFRP is too small. However, when specimens entered the elastoplastic and plastic stage, the impact of AFRP became significant. The stiffness and modulus of reinforced stub columns were much higher than the original columns, because AFRP could effectively curb the development of cracks inside the column. Different from FRP reinforced concrete [16], the positions of initial yield point, and turning points between elastoplastic stage and plastic stage basically remained unchanged. Nevertheless, the ductility of reinforced bamboo columns was much higher. Compared with average ultimate strain value of 0.09 in the reference group, the value in the reinforcement group ranged from 0.106 to 0.16. The obvious strengthening effect of AFRP on the declined elastic modulus and ductility indicates that AFRP sheets have a very high application prospect in seismic reinforcement and retrofit of ancient timber and bamboo buildings.

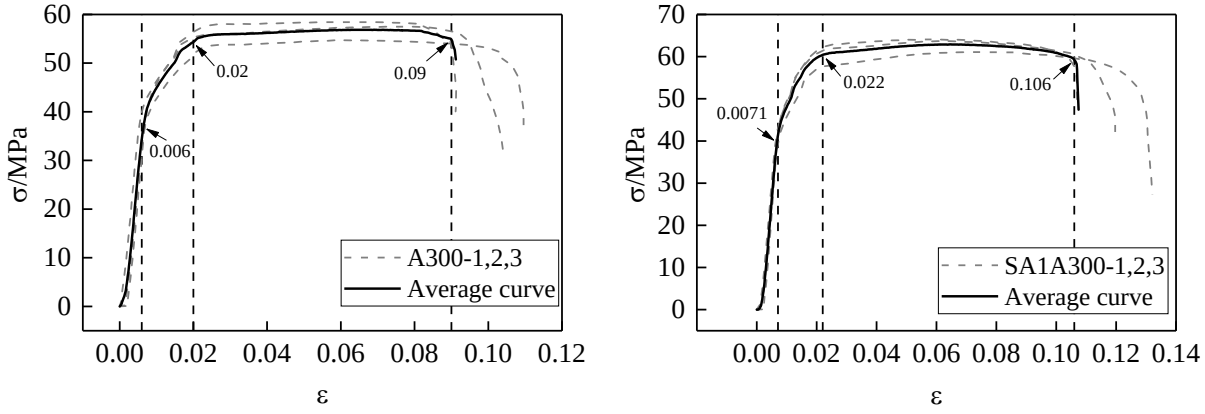

(a) A300

(b) SA1A300

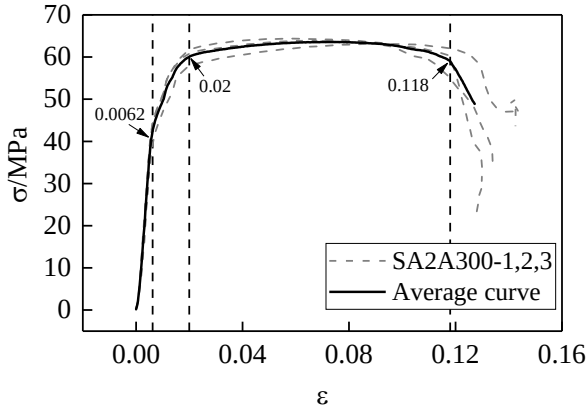

(c) SA2A300

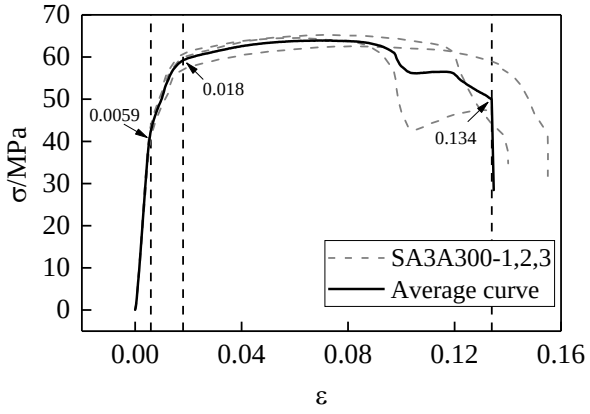

(d) SA3A300

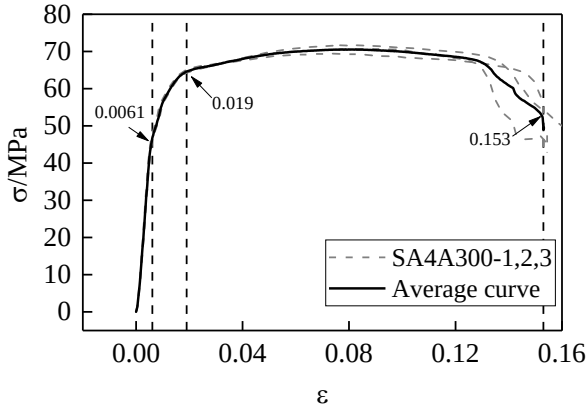

(e) SA4A300

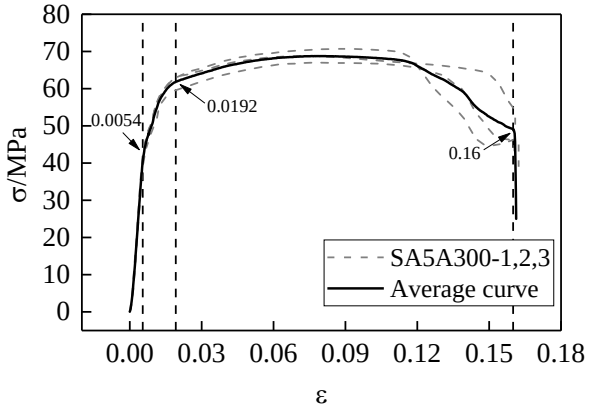

(f) SA5A300

Figure 5 Stress-strain response

In order to accurately fit the constitutive model of bamboo matrix composites, many scholars have proposed a variety of equations with different mathematical functions [29-34]. The existing constitutive models are basically composed of piecewise equations. Each segment of the piecewise equations is generally in the form of a straight line or a parabola, thus the constitutive model can be determined as long as the stress and strain at the end of each stage are given. Referring to the research results of Li et al. [29], the constitutive model of FRP reinforced

laminated bamboo lumber with square section can be described by three-segment linear equation (as shown in Equation 2 and Fig. 6). Where E_1 is initial elastic modulus in the elastic stage, E_2 is reduced elastic modulus in the elastoplastic stage, ε_y is yield strain (0.006), ε_u is ultimate strain corresponding to ultimate strength (0.02), ε_c is maximum strain. Because the values of ε_c are too disperse in the test, theirs exact values and correlation with cloth ratio should be furtherly studied in the future work.

$$\sigma = \begin{cases} E_1\varepsilon & 0 \le \varepsilon \le \varepsilon_y \\ \sigma_y + E_2\left(\varepsilon - \varepsilon_y\right) & \varepsilon_y < \varepsilon < \varepsilon_u \\ \sigma_u & \varepsilon_u \le \varepsilon \le \varepsilon_c \end{cases} \tag{2}$$

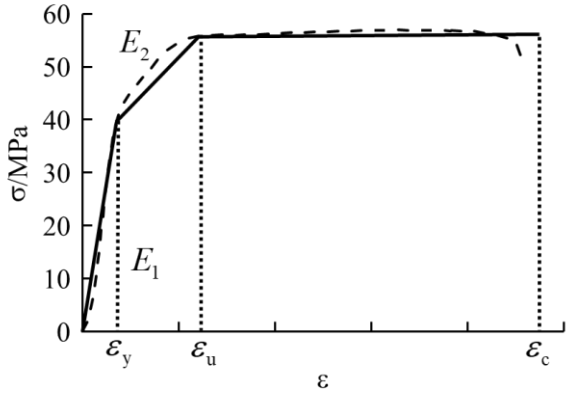

Figure 6 Constitutive model

3.3.3 Ultimate compressive strength

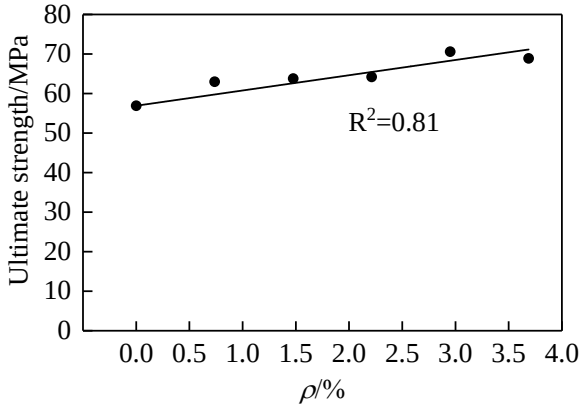

Figure 7 Correlation between ultimate strength and cloth ratio

Fig. 7 shows the correlation between ultimate compressive strength and cloth ratio. It can be seen that the ultimate compressive strength of AFRP reinforced stub columns basically increases linearly with the increase in cloth ratio. By using regression analysis, the relationship between the ultimate compressive strength and the cloth ratio can be described by Equation (3):

$$f_{co}^{'} = 56.9 + 3.91\rho \tag{3}$$

where $f_{co}^{'}$ is the ultimate compressive strength, ρ is the cloth ratio.

3.3.4 Poisson's ratio

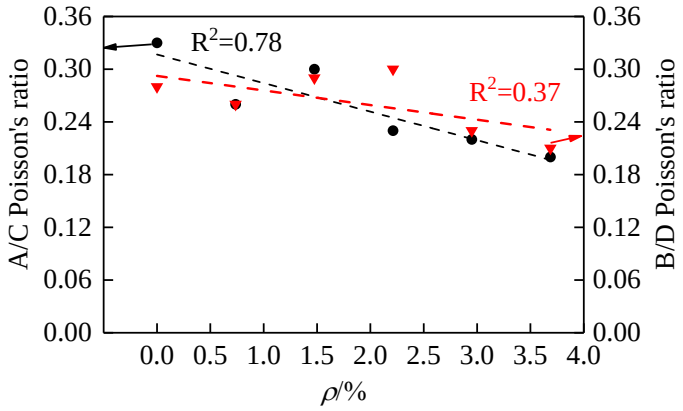

Figure 8 Correlation between Poisson's ratio and cloth ratio

The Poisson's ratio is calculated by dividing the transverse strain by the vertical strain in the elastic stage:

$$\mu = \left| \frac{\varepsilon_{\text{transverse}}}{\varepsilon_{\text{vertical}}} \right| \tag{4}$$

Laminated bamboo lumber is a typical anisotropic bio-based material [5], so the Poisson's ratio is different in A/C and B/D plane. Fig. 8 depicts the correlation between Poisson's ratio and cloth ratio. It is showed that with the increase in cloth ratio, the Poisson's ratio generally decreased, which means the lateral deformation of bamboo columns under compression was effectively restrained by AFRP. Besides, it can be concluded that the lateral deformation was gradually reduced under same load level. By using regression analysis, the relationship between the Poisson's ratio and the cloth ratio can be described by Equations (5) and (6):

$$\mu_{\text{AC}} = 0.33 - 0.038\rho \tag{5}$$

$$\mu_{\text{BD}} = 0.28 - 0.012\rho \tag{6}$$

where μ_{AC} and μ_{BD} are Poisson's ratios, ρ is the cloth ratio. However, due to the highly discrete values of μ_{BD}, Equation (6) is not reliable. It can only show a general change law.

3.3.5 Elastic modulus

Fig. 9a shows the correlation between elastic modulus and cloth ratio, where E_1 means initial elastic modulus and E_2 means reduced elastic modulus in the elastoplastic stage. In general, elastic modulus increases with the increase in cloth ratio. As mentioned before, the thickness and the transverse elastic modulus of AFRP was too small, so that the change of initial stiffness and elastic modulus of AFRP reinforced columns was not very clear. However, these two properties changed a lot when the columns began to yield. Fig. 9b shows relationship between E_1 and E_2. It can be seen that the reduced modulus of stub columns is significantly increased

by applying AFRP. The reference group only retained 10% initial elastic modulus, while the other reinforced groups retained 14%~23% of initial elastic modulus when entering elastoplastic stage.

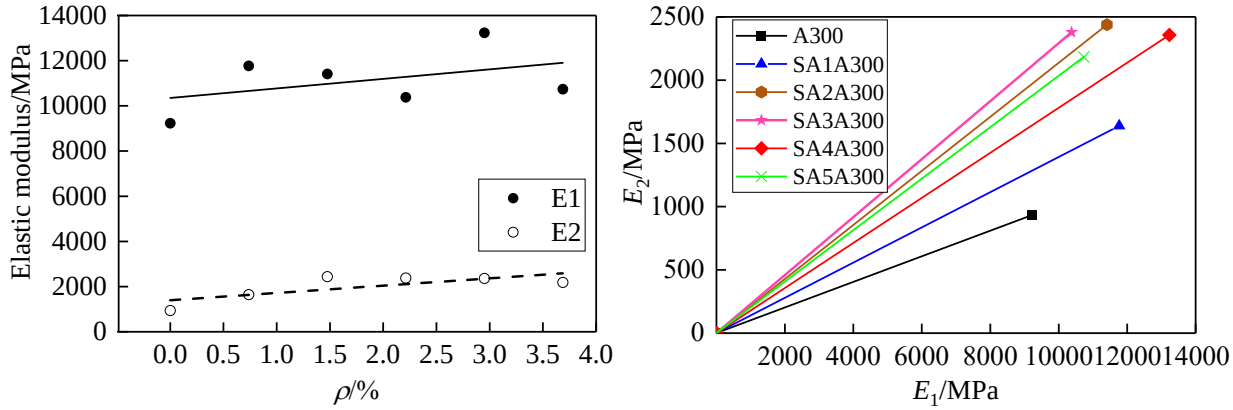

Figure 9 (a) Correlation between E_1, E_2 and cloth ratio (b) Correlation between E_1 and E_2

4 Evaluation of ultimate strength

4.1 Lam and Teng model

In 1996, Retrepol and De Vino [35] proposed an ultimate strength model of FRP reinforced short columns with rectangular section:

$$\frac{f_{cu}^{'}}{f_{co}^{'}} = 1 + k_s k_1 \frac{f_l}{f_{co}^{'}} \tag{7}$$

where $f_{cu}^{'}$ is ultimate compressive strength of reinforced column; f_l is constraint stress; k_s is shape coefficient of cross section, which is defined as the ratio of effective confined zone to cross-sectional area; k_1 is effective constraint coefficient.

Lam and Teng [16] conducted experimental research on FRP reinforced concrete short columns with rectangular section. The proposed functional model is same as Equation (7), while the constraint stress, shape coefficient of cross section and effective constraint coefficient are different. Lam and Teng indicated that the diameter of circumcircle of rectangular section could be used to replace the cylinder diameter in calculating constraint stress:

$$f_l = \frac{2 f_{tu} t_f}{\sqrt{h^2 + b^2}} \tag{8}$$

where, f_{tu} is ultimate tensile strength of FRP; t_f is thickness of FRP; h and b are height and width of rectangular section, respectively.

However, the above two models do not consider the constraint of multi-layer FRP cloth. Therefore, based on the model of Lam and Teng, the ultimate strength model of FRP reinforced laminated bamboo short columns with rectangular section is proposed. Figure 10 depicts the arch action model and calculation diagram of effective area. For columns with rectangular section, the constraint stress at the corner is the largest. The distribution of the constraint stress along the height or width is a quadratic parabola. The effective constraint area is the area surrounded by the arch, and the initial angle of the arch is 45°.

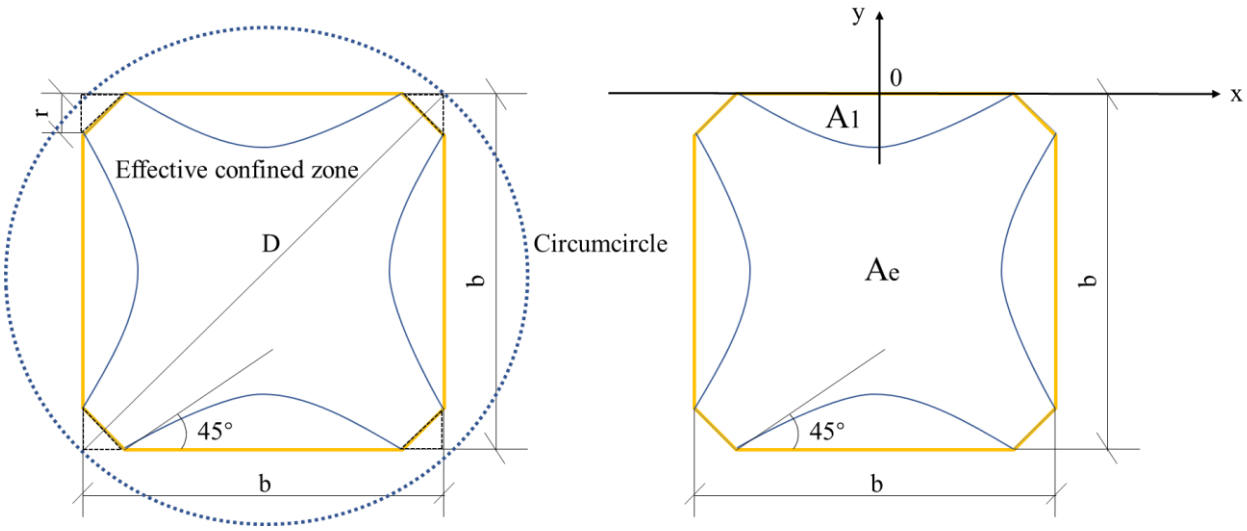

Figure 10 Arch action model and calculation diagram of effective area.

The equation for setting the arch is:

$$y = Ax^2 + C \tag{9}$$

Then the first derivative is:

$$\dot{y} = 2Ax \tag{10}$$

Substituting known conditions $(\frac{b}{2}-r,0)$, $(r-\frac{b}{2},0)$ and $\dot{y}\Big|_{x=\frac{b}{2}-r} = \tan 45^\circ$ into Equations (9~10), the expression of the parabola can be obtained as follows:

$$y = \frac{1}{b-2r}x^2 - \frac{b-2r}{4} \tag{11}$$

The area between the parabola and the edge of the section is:

$$A_1 = -2\int_0^{\frac{b}{2}-r} y dx = \frac{(b-2r)^2}{6} \tag{12}$$

The effective constraint area is then:

$$A_e = A_c - 4A_1 = b^2 - 2r^2 - \frac{2}{3}(b-2r)^2 \tag{13}$$

The shape factor of cross section is:

$$k_s = \frac{A_e}{A_c} = 1 - \frac{2(b-2r)^2}{3(b^2-2r^2)} \tag{14}$$

The correlation between effective constraint coefficient and cloth ratio can be obtained by regression analysis by substituting the sample size and AFRP properties (Fig. 11a). Therefore, the equation for calculating ultimate strength of AFRP reinforced LBL stub columns is:

$$\frac{f_{cu}^{'}}{f_{co}^{'}}=1+1.88\left(1-\frac{2(b-2r)^2}{3(b^2-2r^2)}\right)\rho\frac{f_{tu}t_f}{bf_{co}^{'}} \tag{15}$$

where, ρ is cloth ratio. The results in Fig. 11b and the relative errors less than 6% shown in Table 4 indicate that the calculated results are in coincidence with test results.

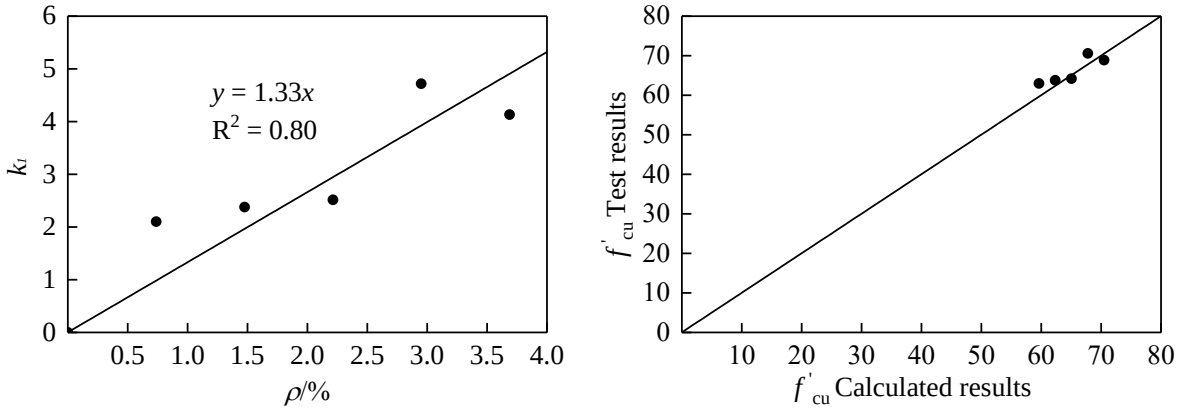

Figure 11(a) Correlation between effective constraint coefficient and cloth ratio (b) Comparison of calculate results and test results

Table 4 Compared results

Group	Test results/MPa	Calculated results/MPa	Relative Error/%
A300	56.9	56.90	0
SA1A300	63.0	59.62	-5.36
SA2A300	63.8	62.34	-2.28
SA3A300	64.2	65.07	1.35
SA4A300	70.6	67.79	-3.98
SA5A300	68.9	70.51	2.34

Note: Relative Error = (Calculated results – Test results) / Test results $\times 100\%$.

4.2 Mises yield criterion

The above models all assume that FRP is fully utilized and use the ultimate tensile strength of FRP directly to calculate ultimate compressive strength. However, it is found from test that the measured stress and strain of FRP was far from its ultimate condition in the small deformation stage, i.e., elastic and elastic-plastic stage. This section attempts to explore the relationship between confining pressure and ultimate compressive strength.

The following three assumptions are used: (1) The deformation between FRP sheets and between FRP and specimens is coordinate, and the bonding condition is perfect; (2) In the elastoplastic stage, the Poisson's ratio of the specimen remains unchanged, which is the same as value in the elastic stage; (3) The confining pressure is evenly distributed along the side of section.

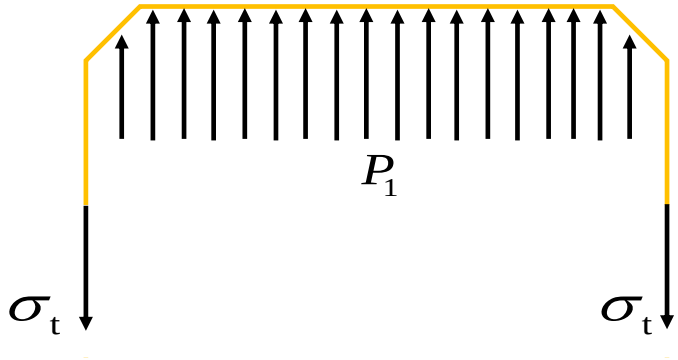

Figure 12 Calculation diagram

According to the principle of force equilibrium (Fig. 12):

$$P_1 b = 2\sigma_t t_f \tag{16}$$

where P_1 is the confining stress on surface A and C; σ_t is the tensile stress caused by deformation of FRP cloth; t_f is the thickness of FRP。Because laminated bamboo lumber is anisotropic material, the stress caused by FRP on A/C and B/D surface is different considering the different Poisson's ratio. Thus P_1 and P_2 can be obtained:

$$P_1 = \frac{2nE_t\mu_{AC}\varepsilon_u t_f}{b} \tag{17}$$

$$P_2 = \frac{2nE_t\mu_{BD}\varepsilon_u t_f}{b} \tag{18}$$

where E_t is elastic modulus of FRP in the fiber direction; μ is Poisson's ratio; ε_u is the ultimate vertical strain corresponding to ultimate compressive strength, which is 0.02. Substituting Poisson's ratio data in Table 3 to Equations (17~18), the confining stress caused by 1~5 AFRP layers on the specimens is shown in Figure 13. Mises failure criterion is:

$$\bar{\sigma} = \frac{1}{\sqrt{2}}\sqrt{(\sigma_1-\sigma_2)^2+(\sigma_2-\sigma_3)^2+(\sigma_3-\sigma_1)^2} \le \sigma_s \tag{19}$$

where $\bar{\sigma}$ is equivalent stress; σ_1, σ_2 and σ_3 are principal stress in three directions; σ_s is material strength obtained from uniaxial compression test, and the value here is 56.9MPa. Substituting the test data into Equation (19) to calculate the equivalent stress, and the results are shown in Figure 14a. It can be seen that the relationship between ultimate compressive strength and confining pressure basically satisfies Mises failure criterion. If the uniaxial compressive strength, Poisson's ratio, ultimate strain, elastic modulus and thickness of FRP are known, the ultimate compressive strength of FRP reinforced LBL stub column can be calculated.

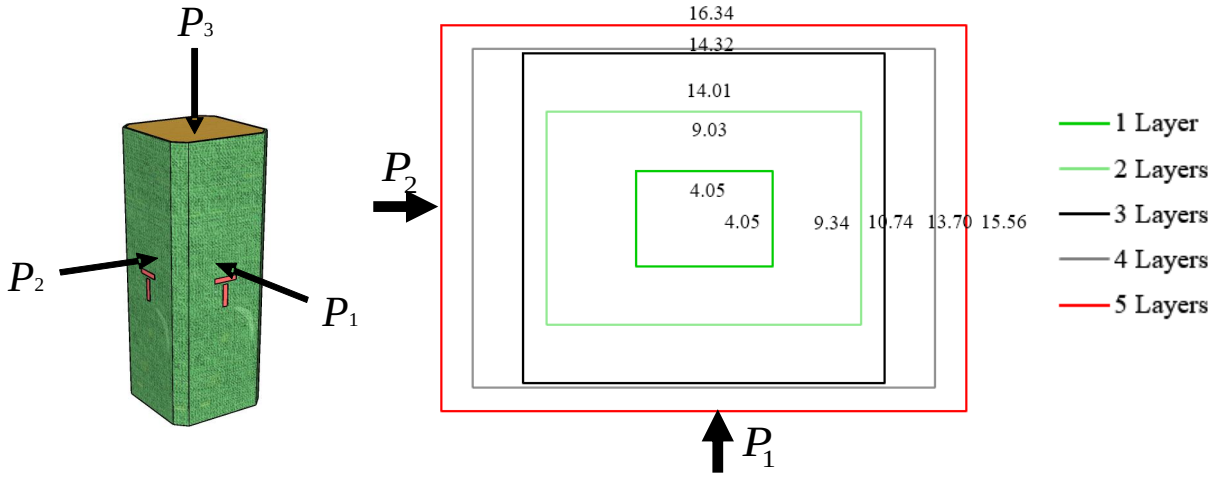

Figure 13 Confining stress caused by 1~5 AFRP layers on the specimens

Although the Poisson's ratios of LBL on surface A/C and B/D are different, they are very close. Assuming they are equal, Equation (19) can be furtherly simplified:

$$\sigma_3 = \sigma_1 + \sigma_s \tag{20}$$

Rewrite Equation (20) to Equation (21):

$$f_{cu}^{'} = f_c + \frac{2nE_t\mu_{AC}\varepsilon_u t_f}{b} \tag{21}$$

Equation (21) means that the ultimate compressive strength of FRP reinforced LBL stub columns can be simplified as the superposition of confining stress and uniaxial compressive strength. From Figure 14b and Table 5, it can be seen that the calculated results are in good agreement with test results and the relative errors are within 6%, which validates the feasibility of proposed equation.

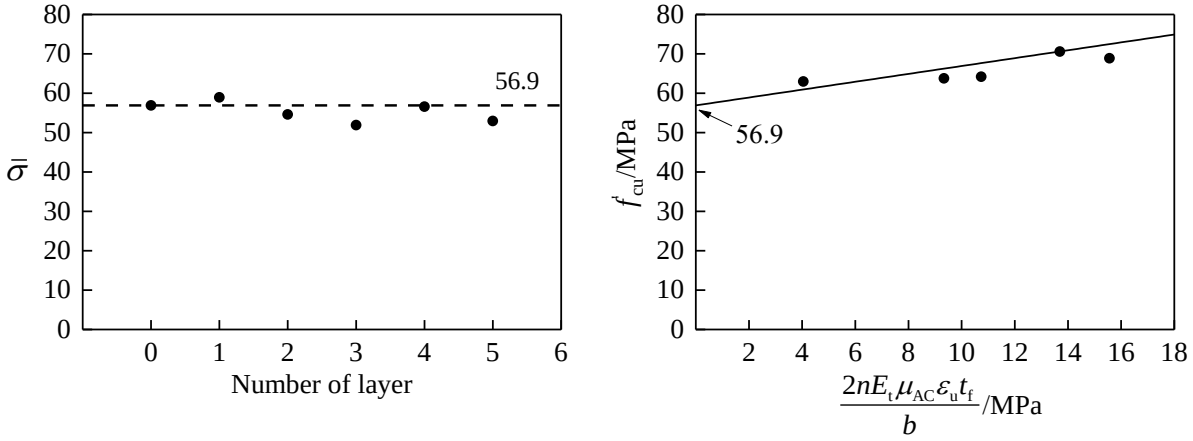

Figure 14 (a) Equivalent stress under different cloth ratio (b) Comparison of calculated results and test results

Table 5 Compared results

Group	Test results/MPa	Equivalent stress/MPa	Calculated results/MPa	Relative Error/%
A300	56.9	56.9	56.90	0
SA1A300	63.0	58.95	60.95	-3.26
SA2A300	63.8	54.62	66.24	3.82

Group	Test results/MPa	Equivalent stress/MPa	Calculated results/MPa	Relative Error/%
SA3A300	64.2	51.90	67.64	4.22
SA4A300	70.6	56.60	70.60	-0.01
SA5A300	68.9	52.95	72.46	5.17

Note: Relative Error = (Calculated results – Test results) / Test results $\times 100\%$.

5 Conclusions

In order to study the compressive behavior of AFRP reinforced laminated bamboo columns, a total number of 18 laminated bamboo columns (6 groups, 3 replicates for each group) were designed and tested according to six cloth ratios i.e. 0%, 0.74%, 1.48%, 2.21%, 2.95% and 3.69%. The following conclusions can be drawn through the test results and analysis:

(1) The failure pattern of unreinforced LBL columns were generally characterized by end crushing with local adhesive damage and bamboo strips cracking. Due to the lateral restriction by AFRP, the reinforced columns failed with tearing of AFRP and cracking in bamboo, without visual crushing at the two ends.

(2) With the increase in cloth ratio, the ultimate strength and elastic modulus increased linearly in general. Although the improvement of initial elastic modulus was rarely, the reduced elastic modulus in the elastoplastic stage was greatly enhanced by AFRP. The Poisson's ratio decreased as cloth ratio increased, which means the lateral deformation of bamboo columns was confined by AFRP.

(3) Although the ductility of bamboo columns wrapped with AFRP was greatly improved, the initial stiffness, proportional limit point and turning points between elastoplastic stage and plastic stage basically remained unchanged. Thus, the existing constitutive models proposed for original laminated bamboo can also be used for reinforced laminated bamboo, if key points are determined.

(4) Considering the effect of cloth ratio, the ultimate strength model of FRP reinforced laminated bamboo short columns was proposed on the basis of test results and 'Lam and Teng' model. However, the existing models assumed that FRP could be fully utilized which was not conformed to fact in the current study. The relationship between confining pressure applied by AFRP and ultimate compressive strength was explored. Based on Mises yield criterion, it was found that the ultimate compressive strength of FRP reinforced LBL stub columns could be simplified as the superposition of confining stress and uniaxial compressive strength.

From the above conclusions, it can be known that FRP actually has little effect on the mechanical properties of new and undamaged engineered bamboo structures. However, the higher value of reduced modulus indicates that applying AFRP on bamboo structures has great potential in the terms of retrofitting structures. Besides, it is also foreseeable that the great improvement of bamboo columns confined with FRP in ductility can prevent danger if earthquake happens to the building. Although FRP has little effect on the mechanical properties in the elastic stage, it may help in the aspect of durability, namely preventing insects and corrosion. The related work should be studied in the future.

Funding: This work was supported by the National Natural Science Foundation of China (No. 51878354 & 51308301); the Natural Science Foundation of Jiangsu Province (No. BK20181402 & BK20130978); Postgraduate Research &Practice Innovation Program of Jiangsu Province; Six talent peak high-level projects of Jiang-su Province (No. JZ-029); and a Project Funded by the Priority Academic Program Development of Jiangsu Higher Education Institutions. Any research results expressed in this paper are those of the writer(s) and do not necessarily reflect the views of the foundations.

Acknowledgment: The writers gratefully acknowledge Zhen Wang, Ben Chen, Xiaoyan Zheng, Shaoyun Zhu, Liqing Liu, Dunben Sun, Jing Cao, Yanjun Liu and others from the Nanjing Forestry University for helping with the tests.
The authors declare that they have no conflicts of interest to this work.

References

[1] Reynolds T, Sharma B, Harries K, et al. Dowelled structural connections in laminated bamboo and timber[J]. Composites Part B: Engineering, 2016, 90: 232-240.

[2] Hong C, Li H, Xiong Z, et al. Review of connections for engineered bamboo structures[J]. Journal of Building Engineering, 2020, 30: 101324.

[3] Qiu Z, Zhu W, Fan H. Flexural performances and failure analyses of parallel bamboo strand lumber plates[J]. Engineering Fracture Mechanics, 2021, 254: 107922.

[4] Xiao Y, Wu Y, Li J, et al. An experimental study on shear strength of glubam[J]. Construction and Building Materials 2017; 150: 490-500.

[5] Shan B, Chen C Q, Deng J Y, et al. Assessing adhesion and glue-line defects in cold-pressing lamination of glubam[J]. Construction and Building Materials, 2021, 274: 122106.

[6] Dauletbek A, Li H, Xiong Z, et al. A review of mechanical behavior of structural laminated bamboo lumber[J]. Sustainable Structures, 1 (1), 2021, 4.

[7] Su J, Li H, Xiong Z, et al. Structural design and construction of an office building with laminated bamboo lumber[J]. Sustain Struct, 2021, 1(2): 000010.

[8] Zhou Y, Huang Y, Sayed U, et al. Research on dynamic characteristics test of wooden floor structure for gymnasium[J]. Sustainable Structures, 1 (1), 2021, 5.

[9] Yang D, Li HT, Xiong ZH, et al. Mechanical Properties of Laminated Bamboo under Off-axis Compression. Composites Part A-Applied Science and Manufacturing 2020; 138: 106042.

[10] Hong C, Li H, Xiong Z, et al. Experimental and numerical study on eccentric compression properties of laminated bamboo columns with a chamfered section[J]. Journal of Building Engineering, 2021, 43: 102901.

[11] Wang Z, Li H, Yang D, et al. Bamboo node effect on the tensile properties of side press-laminated bamboo lumber[J]. Wood Science and Technology, 2021, 55(1): 195-214.

[12] Lv Q, Wang W, Liu Y. Study on Thermal Insulation Performance of Cross-Laminated Bamboo Wall[J]. Journal of Renewable Materials, 2019, 7(11): 1231-1250.

[13] Zhong Y, Ren H Q, Jiang Z H. Effects of temperature on the compressive strength parallel to the grain of bamboo scrimbe[J]. Materials, 2016, 9(6): 436.

[14] Lou Z, Yuan C, Li Y, et al. Effect of saturated steam treatment on the chemical composition and crystallinity properties of bamboo bundles[J]. J. For. Eng, 2020, 5: 29-35.
[15] Lou Z C, Yang L T, Zhang A W, et al. Influence of saturated steam heat treatment on the bamboo color[J]. J For Eng, 2020, 5(4): 38-44.
[16] Teng J G, Chen J F, Smith S T, et al. FRP: strengthened RC structures[M]. 2002.
[17] Abedini M, Zhang C. Dynamic performance of concrete columns retrofitted with FRP using segment pressure technique[J]. Composite Structures, 2021, 260: 113473.
[18] Zhang Y, Wei Y, Bai J, et al. A novel seawater and sea sand concrete filled FRP-carbon steel composite tube column: Concept and behaviour[J]. Composite Structures, 2020, 246: 112421.
[19] Najm H, Secaras J, Balaguru P. Compression tests of circular timber column confined with carbon fibers using inorganic matrix[J]. Journal of materials in civil engineering, 2007, 19(2): 198-204.
[20] Taheri F, Nagaraj M, Khosravi P. Buckling response of glue-laminated columns reinforced with fiber-reinforced plastic sheets[J]. Composite Structures, 2009, 88(3): 481-490.
[21] Kim Y J, Harries K A. Modeling of timber beams strengthened with various CFRP composites[J]. Engineering Structures, 2010, 32(10): 3225-3234.
[22] Zhang W, Song X, Gu X, et al. Compressive behavior of longitudinally cracked timber columns retrofitted using FRP sheets[J]. Journal of Structural Engineering, 2012, 138(1): 90-98.
[23] Premrov M, Dobrila P. Experimental analysis of timber–concrete composite beam strengthened with carbon fibres[J]. Construction and building materials, 2012, 37: 499-506.
[24] Rescalvo F J, Valverde-Palacios I, Suarez E, et al. Experimental and analytical analysis for bending load capacity of old timber beams with defects when reinforced with carbon fiber strips[J]. Composite Structures, 2018, 186: 29-38.
[25] Zhang H, Li H, Corbi I, et al. AFRP influence on parallel bamboo strand lumber beams[J]. Sensors, 2018, 18(9): 2854.
[26] Wang Z, Li H, Fei B, et al. Axial compressive performance of laminated bamboo column with aramid fiber reinforced polymer[J]. Composite Structures, 2021, 258: 113398.
[27] Benmokrane B, Zhang B, Chennouf A. Tensile properties and pullout behaviour of AFRP and CFRP rods for grouted anchor applications[J]. Construction and Building Materials, 2000, 14(3): 157-170.
[28] Toutanji H, Deng Y. Strength and durability performance of concrete axially loaded members confined with AFRP composite sheets[J]. Composites Part B: Engineering, 2002, 33(4): 255-261.
[29] Li H, Su J, Zhang Q, et al. Mechanical performance of laminated bamboo column under axial compression[J]. Composites part B: engineering, 2015, 79: 374-382.
[30] Wei Y, Ji X, Duan M, et al. Flexural performance of bamboo scrimber beams strengthened with fiber-reinforced polymer[J]. Construction and Building Materials, 2017, 142: 66-82.
[31] Shen Y, Huang D, Zhou A, et al. An inelastic model for ultimate state analysis of CFRP reinforced PSB beams[J]. Composites Part B: Engineering, 2017, 115: 266-274.
[32] Chen G, He B. Stress-strain constitutive relation of OSB under axial loading: An experimental investigation[J]. BioResources, 2017, 12(3): 6142-6156.
[33] Qiu Z, Fan H. Nonlinear modeling of bamboo fiber reinforced composite materials[J]. Composite Structures, 2020, 238: 111976.
[34] Zhang H, Li H, Hong C, et al. Size Effect on the Compressive Strength of Laminated Bamboo Lumber[J]. Journal of Materials in Civil Engineering, 2021, 33(7): 04021161.
[35] Restrepol J I, DeVino B. Enhancement of the axial load carrying capacity of reinforced concrete columns by means of fiberglass-epoxy jackets[C]//PROCEEDINGS OF THE 2ND INTERNATIONAL

CONFERENCE ON ADVANCED COMPOSITE MATERIALS IN BRIDGES AND STRUCTURES, ACMBS-II, MONTREAL 1996. 1996.